Microcirculation, 11: 295–306, 2004

ISSN: 1073-9688 print
DOI: 10.1080/10739680490425994

Taylor & Francis
Taylor & Francis Group

Effect of Fibrinogen on Leukocyte Margination and Adhesion in Postcapillary Venules

MARK J. PEARSON AND HERBERT H. LIPOWSKY
Department of Bioengineering, The Pennsylvania State University, University Park, Pennsylvania, USA

ABSTRACT

Objective: To quantitatively evaluate the role of fibrinogen (Fb) as a determinant of leukocyte (WBC) margination in postcapillary venules in light of its ability to induce red blood cell (RBC) aggregation with reductions in shear rate ($\dot{\gamma}$) and increase adhesiveness of WBCs to endothelium (EC).

Methods: Red cell aggregation (RCA), WBC margination (flux at the EC), rolling velocity, and adhesion to the EC were measured in rat mesenteric postcapillary venules upon reducing $\dot{\gamma}$, prior to and following systemic infusion of Fb. Proximal occlusion of feeding microvessels with a blunted probe facilitated reductions in $\dot{\gamma}$ from 600 to 50 s^{-1}. An index of aggregation (G) was derived from light-scattering properties of RBCs, where G was proportional to the number of RBCs per aggregate. WBC margination was measured as the percentage of total luminal WBC flux that rolled on the EC, F^*_{WBC}.

Results: For normal levels of Fb (0.07 g%), reductions in $\dot{\gamma}$ resulted in a 4-fold rise in F^*_{WBC} and no change in G as $\dot{\gamma}$ was reduced to 50 s^{-1}. Infusion of Fb to achieve a plasma concentration to 0.7 g% caused a modest 20% increase in G and a 2.5-fold increase in F^*_{WBC} at $\dot{\gamma} = 50\ s^{-1}$. WBC-EC adhesion appeared to increase significantly, but much less than with infusion of high molecular weight dextran (Dx). With Dx, G increased 3-fold, with reductions in $\dot{\gamma}$, but F^*_{WBC} increased only half the amount incurred with Fb at low shear. The greater margination in the presence of Fb results from RBC rouleaux that promote radial migration of WBCs. In contrast, clumps of RBCs resulting from high molecular weight Dx entrain WBCs within plasma gaps along the vessel centerline.

Conclusions: In the presence of Fb, margination of WBCs increases dramatically at low shear due to rouleaux formation, which enhances radial migration of WBCs. This effect is much greater than with Dx because disruption of the much weaker Fb induced rouleaux precludes reductions in H_{MICRO}, whereas clumping aggregates induced by Dx form plasma gaps. Thus, modest levels of RCA caused by increased Fb may greatly enhance margination and with an enhancement of adhesiveness synergistically promote firm WBC-EC adhesion in the low flow state.
Microcirculation (2004) **11,** 295–306. doi:10.1080/10739680490425994

KEY WORDS: erythrocyte aggregation, fibrinogen, leukocyte–endothelium adhesion, leukocyte margination, rat mesentery

INTRODUCTION

Fibrinogen, well known for its role in thrombosis and hemostasis, is recognized as an important ligand between blood cellular elements. It is the principal bridge between adherent platelets with specificity for the gp IIb/IIIa receptor on the platelet membrane (7). In concert with the large serum globulins, it is responsible for erythrocyte aggregation attendant to reductions in shear rate (5), and has also been found to support white blood cell (WBC) adhesion to the endothelium (EC) by serving as a ligand between ICAM-1 (CD54) on ECs and Mac-1 (CD11b/CD18) on leukocytes (16,17). Thus, because of its major contribution to red cell aggregation (RCA) and WBC-EC adhesion it may play an important role as a determinant of the sequence of WBC margination, rolling, and firm adhesion that precede WBC diapedesis in the inflammatory process.

As blood exits the true capillary network, the radial migration of WBCs toward the postcapillary EC (margination) revolves around the dynamic interactions between RBCs and WBCs that result in a phase

The authors thank Karen Trippett for her technical assistance. This work was supported by NIH Research Grant HL-39286.

Address correspondence to Dr. Herbert H. Lipowsky, Department of Bioengineering, Penn State University, 205 Hallowell Building, University Park, PA 16802, USA. E-mail: HHLBIO@engr.psu.edu

Received 23 April 2003; accepted 22 August 2003.

separation of RBCs and WBCs (30). Individual red cells and aggregates of red cells tend to displace the WBC toward the venular wall, thus promoting the initial contact between WBC and EC that leads to sustained rolling and subsequent firm adhesion. Using techniques to induce RCA with the polysaccharide dextran, *in vitro* studies (11,24) have demonstrated enhanced margination in response to RCA in small-bore glass tubes. The observation of enhanced margination arising from amplified RCA has long been observed *in vivo* by intravital microscopy (33). However, the lack of suitable techniques to quantitatively assess the extent of RCA has hindered an evaluation of its role in affecting WBC-EC contact. To overcome these limitations, recent studies have employed optical techniques to derive quantitative correlates between RCA and margination in response to high molecular weight dextrans (27). By measurement of the light scattering of red cell aggregates at multiple wavelengths, a measure of the effective size of the light scattering particles was used to define an index of aggregation that could be readily obtained in postcapillary venules of the mesenteric microcirculation. Inducing a threefold increase in RCA at low shear rates with high molecular weight dextran resulted in an almost twofold increase in the rolling flux of WBCs at the venular wall, and disaggregation with low molecular weight dextran resulted in a two-thirds reduction in rolling flux. Concomitant increases in firm WBC-EC adhesion positively correlated with RCA, presumably due to the enhanced probability of WBC-EC contact arising from sustained rolling caused by RCA.

Elevated levels of fibrinogen have long been identified as a risk factor for the onset of cardiovascular disease (9), and have been associated with numerous disorders, such as inflammation (3,31), hypertension (18), coronary heart disease, and atherosclerosis (19). The risk of cardiovascular disease has been positively correlated with elevated fibrinogen levels in a range of 0.13–0.70 g% (15). Hence, an assessment of the effectiveness of fibrinogen induced RCA in modulating WBC margination may provide new insights into the pathogenesis of these disorders. Within this framework, an exploration is presented here of the underlying hypothesis that elevated fibrinogen levels may promote WBC-EC interaction through enhanced margination arising from its effect on RCA, and increased WBC rolling due to enhanced adhesive interactions. To this end, systemic fibrinogen levels were increased by infusion via the jugular vein, and the extent of RCA in mesenteric venules was measured over a physiologically relevant range of wall shear rates by gently occluding proximal arterioles with a blunt probe. Quantitative measures of the degree of aggregation were obtained by spectrophotometric measurement of the light scattering properties of red cells within the venules. These data were contrasted to levels of RCA attained *in vivo* with high molecular weight dextrans to interpret these results in light of levels of RCA typically studied by *in vitro* viscometry.

METHODS

Male Sprague–Dawley rats (367 ± 51 g) were anesthetized with sodium pentobarbital (35 mg/kg, ip). Following tracheostomy, a jugular vein and carotid artery were cannulated with polyethylene tubing for infusions of supplemental anesthetic or fibrinogen and for monitoring systemic arterial pressure or removing blood samples, respectively. The intestinal mesentery was exteriorized and suffused with warmed (37 ± 1°C) HEPES-buffered Ringer's (4.20 mM HEPES, 0.126 M NaCl, 22.85 mM $NaHCO_3$, 3.43 mM KCl, 10.5 mL 2.75% w/v $CaCl_2$) with 1% 275 bloom Gelatin (Fisher), pH 7.4. An intravital microscope, with transillumination from a 150-W xenon lamp, 13×/0.22 NA objective and 10× eyepiece, was used to view vessels in a selected segment of the mesentery. A single postcapillary venule (53 ± 11 SD μm diameter) far (>1000 μm) from inlets or outlets was selected for observation. A blunted micropipette, held in a micromanipulator, was used to gently compress a proximal arteriole to reduce wall shear rates ($\dot{\gamma}$)

RBC velocities (V_{RBC}) were measured along the vessel center line by the 2-slit photometric technique (34), and mean velocities (V_{MEAN}) were obtained from the empirical relationship $V_{RBC}/1.6$ (2). Luminal diameters (D) were measured by the video image shearing method (IPM, model 908) (12). Wall $\dot{\gamma}$ was calculated as for a Newtonian fluid (i.e., $\dot{\gamma} = 8\ V_{MEAN}/D$).

Hematocrit, WBC counts, and differential WBC counts were measured for blood samples removed from the rat. High concentration (~4 g%) fibrinogen stock solutions were prepared by slowly dissolving 1 g porcine fibrinogen (Sigma) in 10 mL Phosphate-buffered saline (PBS) (Sigma) at 37°C, pH 7.4. This solution was then centrifuged at 2500 rpm for 10 min to remove any precipitates, and the remaining solution was dialysed overnight against PBS to remove any impurities. The centrifugation was repeated to remove any additional precipitates. The final

solution was stored in 1.8-mL aliquots at −20°C until needed. The concentration of fibrinogen stock solutions was measured using the thrombin clotting technique (29); absorption was measured at 280 nm on a Shimadzu UV-160A spectrophotometer.

Fibrinogen solutions were tested for the presence of endotoxin using the gel-clot Limulus assay (Biowhitaker), and were found to range from 4 to 4000 EU/mL. To determine if the upper limit of endotoxin has a significant effect, separate experiments were conducted to measure changes in the flux of WBCs that rolled along the endothelium in mesenteric postcapillary venules following an equivalent endotoxin challenge. Flux was measured as a function of time following systemic administration of 7.3 μg/kg LPS from *E. coli* serotype 0127:B8 (Sigma-Aldrich). Regression analysis of flux F vs. time t revealed no significant change for 6 venules over a 60-min postinfusion period, with $F/F_{\text{PREINFUSION}} = 1.014 + 0.00533\times\ t$, $R^2 = 0.0716$, and $p = .206$ (t test of R). Thus, the short duration of these experiments precluded adverse effects due to endotoxin contamination. The dextran solutions used for comparison, had no detectable endotoxin (<0.25 EU/mL).

For study of the effects of RCA on WBC margination, hemodynamic measurements were made before and after a single isovolemic exchange of blood with 1.8 mL fibrinogen stock solution, warmed to 37°C. Plasma fibrinogen levels were measured before and after fibrinogen exchange by the thrombin clotting technique (29), and found to increase 8-fold. RCA measurements were made at a series of shear rates $\dot{\gamma}$ before and after the fibrinogen exchange, and flow at each shear rate was recorded on video for approximately 3 min for off-line analysis. The video recordings were used to count the flux of WBCs rolling or sticking to the wall and to calculate the average WBC rolling velocity V_{WBC}.

Microvessel hematocrit H_{micro} and an index of aggregation G were derived from optical density (OD) measurements of postcapillary venules measured in real time at 2 isobestic wavelengths, 520 and 546 nm. H_{micro} was calculated from the difference in optical densities at these 2 wavelengths (22) and vessel diameter (D) as $H_{\text{MICRO}} = K\,\Delta\text{OD}/D$, where $\Delta\text{OD} = \text{OD}_{546} - \text{OD}_{520}$, and K is a constant of proportionality. As shown previously (22), H_{MICRO} corresponds to the tube hematocrit, defined as the percentage of packed cells that occupy the vessel at any instant of time, in contrast to the discharge hematocrit, which represents that value obtained by collecting the effluent of the tube.

The index of aggregation G was calculated from the magnitude of the scattering component (OD_{SCAT}) of the total optical density (OD_{TOTAL}), assuming that the latter equals the sum of OD_{SCAT} and an absorption component, OD_{ABS}, i.e., $\text{OD}_{\text{TOTAL}} = \text{OD}_{\text{SCAT}} + \text{OD}_{\text{ABS}}$. Derivation of G has been described previously (27). In brief, OD_{SCAT} may be assumed equal at 2 closely spaced wavelengths and may be determined from the measured $\text{OD}_{\text{ABS520}}$ and $\text{OD}_{\text{ABS546}}$ by taking advantage of the fact that the ratio of molecular extinction coefficients of hemoglobin at these wavelengths is approximately 2, to yield the relationship that $\text{OD}_{\text{SCAT}} = \text{OD}_{\text{ABS},520} - \Delta\text{OD}$. The index of aggregation may then be derived using Twersky's theory for the light scattering of large particles of a given diameter and volume (32) to obtain the relationship

$$\text{OD}_{\text{scat}} = -\log\left[1 - (1 - q_0)G^{-\frac{2}{3}}\left(1 - 10^{-a_0 G^{\frac{1}{3}}X}\right)\right] \tag{1}$$

where a_0 and q_0 are parameters dependent on the numerical aperture of the microscope objective, the indices of refraction of the suspending medium and red cells, and wavelength. X represents the contribution of hematocrit and optical pathlength (diameter) and is defined as $X = D(H_{\text{MICRO}} - H^2_{\text{MICRO}})$. Values for a_0 and q_0 were obtained for a nonaggregating RBC suspension in Ringer's solution while flowing through glass tubes at high shear rate (22). To compensate for differences in index of refraction between the glass tubes and *in vivo* microvessels, values of a_0 and q_0 were adjusted to yield a value of $G = 1$ in postcapillary venules at shear rates above 350 s^{-1}, as detailed previously (27). Values of G corresponding to measurements of OD_{SCAT}, H_{MICRO}, and D were obtained from equation 1 by the iterative Newton–Raphson method. Under idealized conditions of a suspension of aggregates composed of spherical particles of a given diameter, G represents the number of particles per aggregate. Thus, for a completely dissagregated state, $G = 1$ implies one red cell per aggregate, and as aggregation proceeds, G takes on a value proportional to the number of particles per aggregate.

WBC margination was quantified as the percentage of total WBC volumetric flux that rolled along the venular wall, F_{WBC} as defined previously (10). This parameter was calculated as the ratio of the flux of WBCs rolling along the wall (f_{WBC}, cells/s) to the

potentially maximum convective WBC flux within the lumen of a microvessel, f_{MAX}. Luminal WBC flux (f_{MAX}) was calculated from the product of bulk volumetric flow rate ($Q = V_{MEAN}\pi D^2/4$) and systemic leukocyte count [WBC_{SYS}], cells per unit volume (obtained by Coulter counter), and the ratio of f_{WBC}/f_{MAX} was calculated as

$$F_{WBC} = \frac{f_{WBC}}{[WBC_{SYS}]V_{MEAN}(\pi D^2/4)} \qquad (2)$$

The variation of F_{WBC} among the ensemble of microvessels studied was minimized by normalizing with respect to its value at high wall shear rates of $\sim 450\ s^{-1}$, i.e., $F^*_{WBC} = F_{WBC}/F_{WBC,\dot{\gamma}=450\,s^{-1}}$.

RESULTS

Systemic Effects of Fibrinogen Infusion

The effects of the fibrinogen (Fb) infusion protocol on systemic hemodynamics were assessed in terms of changes in systemic arterial pressure (P_{art}). In comparison to administering dextran 500 (Dx500) in Sprague–Dawley rats, where P_{art} dropped by 50% following infusion due to an anaphylactic reaction (13), fibrinogen caused no such drop. Approximately 2 mL blood was removed via the carotid artery and used to measure hematocrit, WBC counts, and fibrinogen concentration. This withdrawal of blood resulted in a significant drop in P_{art} from 135 ± 9 to 95 ± 26 mm Hg (SD). This volume of blood was slowly replaced with fibrinogen stock solution

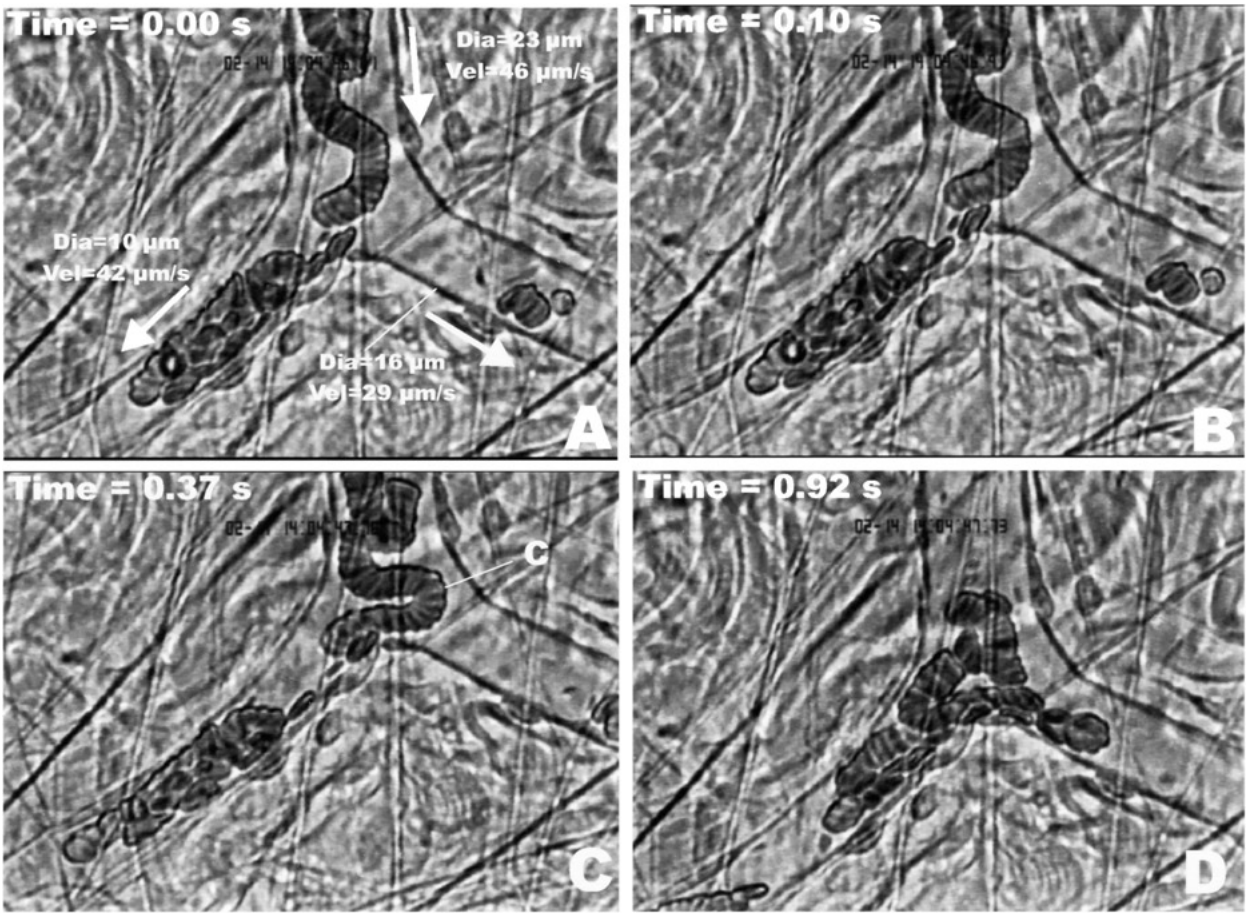

Figure 1. Sequential photographs during a 1-s period of time (A–D) of RBC aggregates flowing slowly through a precapillary bifurcation following administration of fibrinogen. Fibrinogen results in formation of large rouleaux, in contrast to clumps of RBCs formed by Dx500 as seen in Figure 2. Red cell velocities and vessel diameters are indicated for each branch. As the rouleaux enter the branch they are easily deformed as they impact the wall at the bifurcation point and tend to coil up (c) resulting in larger aggregates that are eventually broken apart as flow enters the daughter branches.

(~4 g%), following which P_{art} recovered to 126 ± 20 mm Hg (SD) within 5 min. The recovered P_{art} was not significantly different (paired t test, $p > .12$) to the preinfusion value. Following this isovolemic exchange, the animal was allowed to stabilize for 15 min prior to making hemodynamic measurements in venules.

To determine if fibrinogen resulted in WBC activation, the nitro-blue tetrazolium test (25) was performed on blood samples taken from the carotid artery. No evidence of WBC activation was found in either blood samples taken after fibrinogen was infused and allowed to circulate for 1 h or with *in vitro* samples of WBCs incubated with 0.8 g% fibrinogen for 1 h.

Venular Hemodynamics in Response to Fibrinogen Infusion

The aggregating effect of the infused fibrinogen is illustrated in Figure 1 for a sequence of video frames digitized over a 1-s period at 4 discrete time intervals during reductions in shear rate induced by a proximal partial occlusion of the feeding arteriole. Fibrinogen resulted in the formation of red cell rouleaux, in contrast to the clumping-type aggregation common with Dx500 (Figure 2). The formation of rouleaux compared to clumps is indicative of the lesser strength of the adhesive bonds between aggregates with fibrinogen. Flow velocities and microvessel diameters are shown for parent and daughter branches of the bifurcations shown in Figures 1 and 2. In Figure 2, a tether can be seen between two aggregating RBCs. Tethers were often found after either fibrinogen or Dx500 infusion. However, at 0.74 ± 0.24 g% fibrinogen, much weaker tethers formed than for 3.0 g% Dx500. The stronger tethers with Dx were indicated by greater deformations of RBCs during the disruption of tethered aggregates, a longer time to disrupt tethers, and a longer length of the tether at the moment of rupture. Microscopic *in vitro* observations of RBCs suspended in various concentrations of Fb up

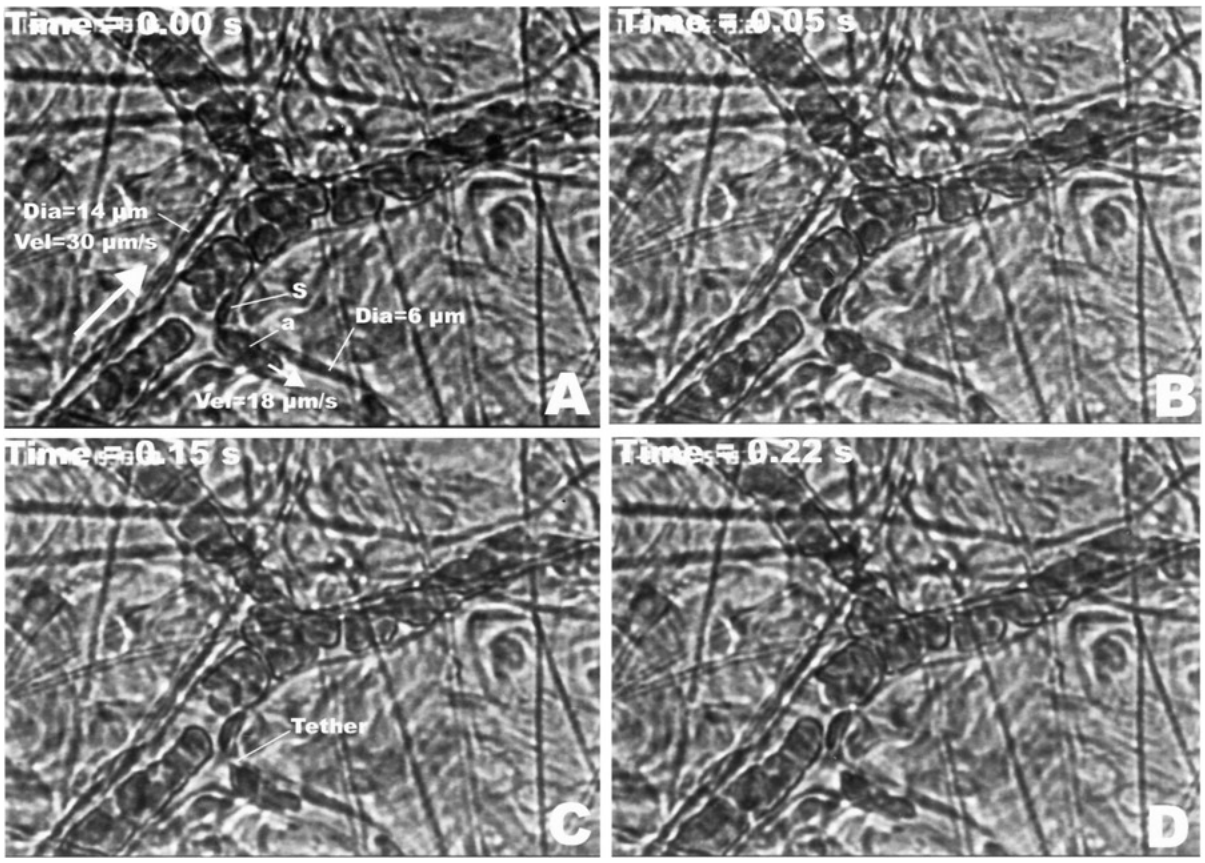

Figure 2. Sequential photographs in time (A–D) of rat RBCs flowing through a precapillary bifurcation after aggregation was enhanced by iv infusion of Dx500. Clumping-type aggregates (a), which tend to bind the RBCs more vigorously compared to the fibrinogen (Figure 1), can be seen that must be broken apart to permit RBCs to pass through the capillaries. A tether formed between a stationary RBC (s) and an aggregate (a) that moves slowly away is seen in A–C, and breaks in D, thus signifying the greater strength of aggregates formed with Dx.

to 3 g% revealed increasing numbers of tethers at higher Fb concentrations.

Shown in Figure 3 is the time course of microvessel hematocrit (H_{MICRO}, RBC velocity V_{RBC}), and shear rate $\dot{\gamma}$ in postcapillary venules before and after infusion of fibrinogen. Circulating fibrinogen levels were increased from 0.09 ± 0.08 (control) to 0.74 ± 0.24 SD g%. For 1 h prior to and following the infusion, all parameters remained invariant with time (t test on regression slope, $p > .42$). There was a small (12%) drop in H_{MICRO} following the fibrinogen infusion. Also shown in Figure 3 are data (dotted lines) for 3.0 ± 0.5 g/dL Dx500 from a previous study (27) as a comparison. When Dx500 was infused, H_{MICRO} decreased by 35%. For both Dx500 and fibrinogen, V_{RBC} and $\dot{\gamma}$ changed by a similar amount.

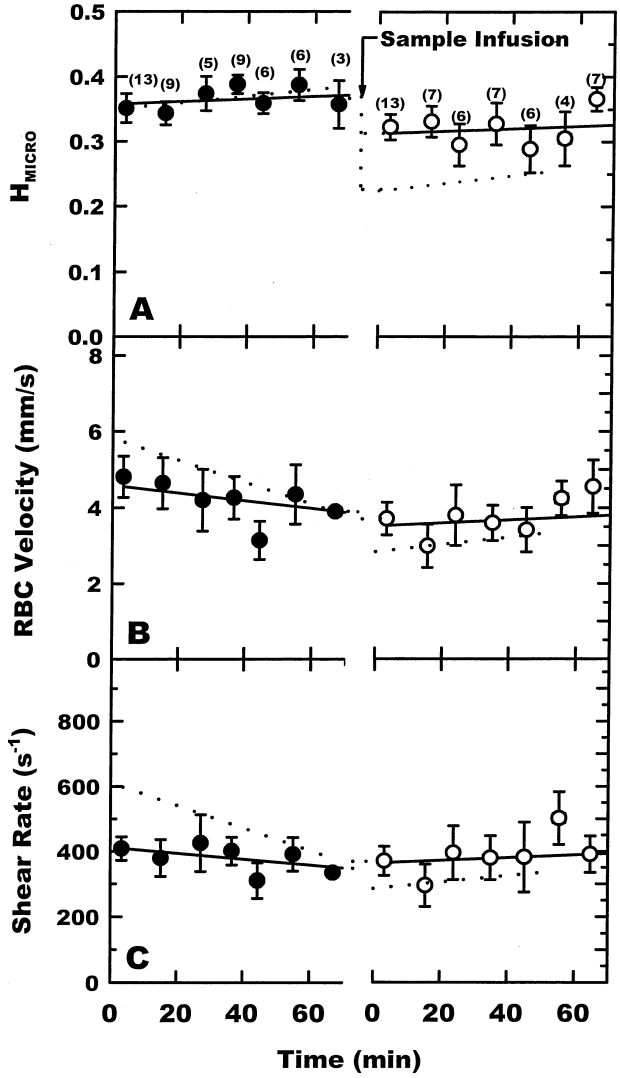

Figure 3. Microvessel hematocrit (H_{MICRO}), red cell velocity, and shear rate, before (●) and after (○) a single intravenous infusion of fibrinogen (by isovolemic exchange) to attain a systemic concentration of 0.72 g%. H_{MICRO} did not change significantly (t test on slopes, $p > .50$) with time either before or after the infusion of fibrinogen. Also shown (dotted curve) are the data obtained after Dx500 infusion, which results in a significant drop in H_{MICRO} ($p < .05$). Shown are the means ± SE of the number of measurements indicated in parentheses for a total of 12 postcapillary venules.

A summary of hemodynamic parameters for all venules studied is shown in Table 1. Following fibrinogen infusion, venule diameters were unchanged (paired t test, $p > .34$). Prior to the microocclusion to induce a low-flow state, V_{RBC} and $\dot{\gamma}$ decreased significantly (paired t test, $p < .011$) with infusion of fibrinogen, and systemic WBC count also dropped significantly by 36% (paired t test, $p < .001$). WBC differential counts showed a significant (paired t test, $p < .001$) increase in neutrophils from 24.1 ± 7.0 to 49.2 ± 18.1% and decrease in lymphocytes from 73.9 ± 7.6 to 50.2 ± 18.0% of total. This decline in WBC count resulted in a 55% drop in the potentially maximum WBC flux within the vessel (calculated with equation 2). In contrast, the marginating WBC flux increased by 29%. Changes in V_{RBC} and $\dot{\gamma}$ with Fb were similar to those observed previously with Dx500 (27). However, systemic and microvessel hematocrits dropped more substantially with Dx500, and systemic WBC count dropped substantially less. With Dx500, the marginating flux did not change after infusion (27), suggesting a lesser increase in WBC margination than observed with fibrinogen.

A comparison of WBC rolling velocity (V_{WBC}) and shear rates is presented in Figure 4 for data grouped at high shear rates (>350 s^{-1}), and low shear rates (<250 s^{-1}) induced by the microocclusion protocol. Following fibrinogen infusion, V_{WBC} decreased significantly by 16% at low and 38% at high $\dot{\gamma}$, which was not as great as when Dx500 was used where a decrease of 39 and 49% was observed respectively (Figure 4A). To account for the diminished shearing forces acting on the WBC with reductions in shear rate, the ratio of V_{WBC} to $\dot{\gamma}$ was taken as a measure of the strength of the adhesive interaction between WBC and EC (Figure 4B). This parameter showed a drop of 10% at low $\dot{\gamma}$ and 35% at high $\dot{\gamma}$, which was not as great as observed with Dx500, where a drop of 32% at low $\dot{\gamma}$ and 46% at high $\dot{\gamma}$ was observed. Following fibrinogen infusion WBC adhesion (per 100 μm vessel length) increased by 70 and 102% at low and high $\dot{\gamma}$, respectively, whereas Dx500 caused a greater

Table 1. Hemodynamic parameters in response to infusion of fibrinogen

	Venule diameter (μm)	RBC velocity (mm s^{-1})	Wall shear rate (s^{-1})	H_{SYS} (%)	H_{MICRO} (%)	[WBC_{SYS}] (cells/mm^3)	Max luminal flux (cells/min)	Marginating Flux (cells/min)	Fraction of luminal WBC flux $F_{M\ WBC}$ (%)	Normalized margination index F^*_{WBC}
Preinfusion	52.9 ± 11.0	4.5 ± 2.0	424 ± 160	48.3 ± 2.6	35.9 ± 5.3	9704 ± 2949	3861 ± 2796	23.2 ± 13.4	0.98 ± 1.01	1.47 ± 1.38
Postinfusion	52.8 ± 11.2	3.5 ± 1.6	342* ± 160	45.0 ± 2.6	35.3 ± 7.3	6167* ± 2869	1728* ± 1207	30.0 ± 9.1	2.67* ± 2.21	5.42* ± 5.73

Note. Shown are hemodynamic parameters and maximum lumen and average marginating WBC fluxes (mean ± SD), measured in 12 venules, and the fraction (F_{WBC}) of the lumen flux as defined by equation 2. F^*_{WBC} is the WBC flux, normalized to its preinfusion (Fb or Dx) value at high $\dot{\gamma}$.
*Significant difference between pre- and postinfusion values, $p < .05$.

increase of 94 and 311%, respectively (Figure 4C). At low and high values of $\dot{\gamma}$, the normalized fractional flux of marginating WBCs (F^*_{WBC}) increased significantly with increased Fb, but to a lesser extent following Dx500 (Figure 4D).

When sulfated Dx500, known to inhibit WBC rolling (20), was infused ~60 min after the fibrinogen sample, at a concentration of 0.03 g%, systemic WBC counts were seen to rise again to their preinfusion levels. This behavior suggests that the increase in the number of rolling WBCs, was consistent with an increase in the marginating pool and a concomitant decrease in systemic WBC count.

Effects of Reductions in $\dot{\gamma}$, RCA, and WBC Margination

With reductions in $\dot{\gamma}$, the extent to which RCA affected the radial migration of WBCs was markedly different for Fb and Dx, as illustrated in Figure 5 for an induced low-flow state ($\dot{\gamma} < 50\ s^{-1}$). The rouleaux resulting from Fb served to exclude WBCs from the axial core and maintain their rolling contact with the EC (Figure 5A). In contrast, the clumps of cells formed in the presence of Dx promoted the formation of plasma gaps, within which WBCs became entrained and sequestered along the vessel centerline (Figure 5B).

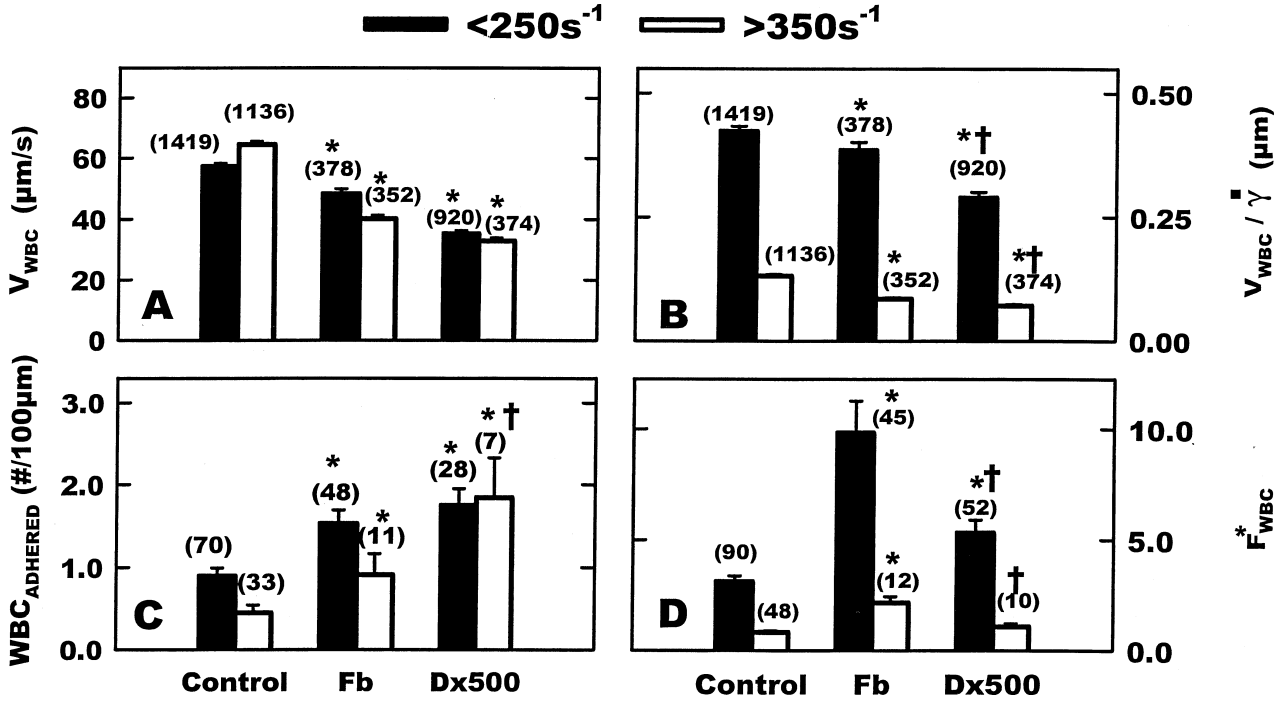

Figure 4. (A) WBC rolling velocity (V_{WBC}), (B) V_{WBC} normalized with respect to prevailing shear rates, $\dot{\gamma}$, (C) the number of WBCs adhering to the endothelium per 100 μm venule length ($WBC_{ADHERED}$), and (D) the WBC marginating flux, normalized with respect to flux at $\dot{\gamma} = 450\ s^{-1}$ ($F^*_{WBC} = F_{WBC}/F_{WBC,\gamma=450}$); at low ($\dot{\gamma} < 200\ s^{-1}$) and high ($\dot{\gamma} > 350\ s^{-1}$) shear rates, before and after fibrinogen or Dx500 (27) infusion. The bars indicate means ± SE and the number of measurements are given in parentheses. *Significantly different from control using Mann–Whitney rank sum test ($p < .001$); †significant difference between Dx and Fb.

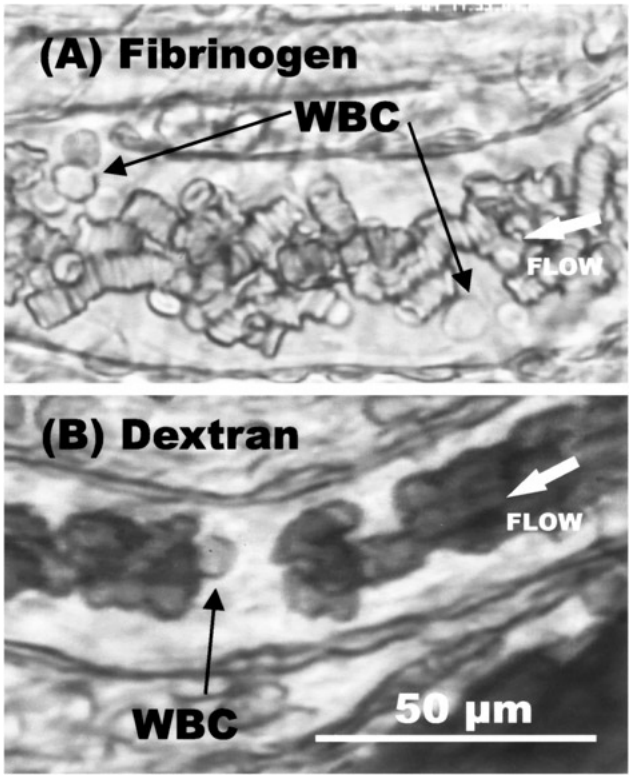

Figure 5. Illustration of the distribution of RBC aggregates and WBCs in postcapillary venules during an induced low flow state ($\dot{\gamma} < 50\ s^{-1}$), with (A) fibrinogen (0.7 g%) and (B) 500 kDa dextran (3 g%). The red cell rouleaux formed by fibrinogen served to exclude WBCs from the axial core and promote their radial migration toward the endothelium. The clumps formed by dextran resulted in numerous plasma gaps which entrained WBCs along the venule centerline.

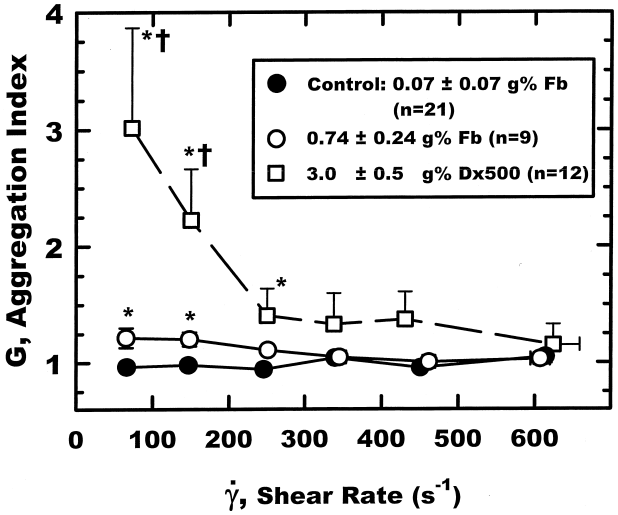

Figure 6. Variation of the aggregation index (G) with reductions in wall shear rate ($\dot{\gamma}$) for the indicated plasma concentrations of fibrinogen (solid) or Dx500 (dashed) (27). Control measurements of G for native plasma with [Fb] = 0.07 g% (●) did not change significantly with reductions in $\dot{\gamma}$ induced by a blunted microprobe. Infusion of either fibrinogen (○) or Dx500 (□) resulted in significant increases in G as $\dot{\gamma}$ was reduced below 350 s^{-1}. *Significantly different from control using Mann–Whitney rank sum test, $p < .04$. †Significant difference between Dx500 and Fb data ($p < .05$). Each point represents the mean ± SE.

To illustrate the graded variation of RCA with reductions in shear rate, *in vivo* measurements of the aggregation index G with reductions in $\dot{\gamma}$ are shown in Figure 6. Prior to the Fb infusion its circulating autologous level equaled 0.07 g% and G remained unchanged with reductions in $\dot{\gamma}$ from 600 to 50 s^{-1}, suggesting little or no RCA. Following fibrinogen infusion, G was significantly increased by 20% as $\dot{\gamma}$ cell below 250 s^{-1} (rank sum test, $p < .04$). Also shown in Figure 6 are the prior results (27) using Dx500 (dashed line), which demonstrate a much larger (200%) increase in RCA for Dx500, compared to Fb below 250 s^{-1}. With Dx500, the level of RCA was significantly greater than that following infusion of Fb for shear rates less than or equal to 150 s^{-1}.

The corresponding normalized index of WBC margination (F^*_{WBC}) is shown in Figure 7. Prior to fibrinogen infusion (Fb = 0.09 g%), F^*_{WBC} increased as $\dot{\gamma}$ decreased from ~600 to 50 s^{-1}. After fibrinogen infusion (Fb = 0.71 g%), F^*_{WBC} was elevated compared to preinfusion levels at all $\dot{\gamma}$ and increased much more rapidly as $\dot{\gamma}$ was reduced below 150 s^{-1} ($p < .001$, rank sum test). Below this shear rate, the margination remained constant ($p > .69$, rank sum test). Also shown is F^*_{WBC} after infusion of Dx500 (dashed line), where it appears that F^*_{WBC} does not rise with reductions in $\dot{\gamma}$ as rapidly as for fibrinogen, and only increased from control below 350 s^{-1}. Thus, fibrinogen induced far more WBC margination than Dx500 at all $\dot{\gamma}$.

DISCUSSION

The present study of the influence of RCA on WBC margination addresses 2 fundamental determinants of the resistance to blood flow in the microcirculation: RCA, which acts through the increase in bulk viscosity of the suspension with reductions in shear rate (5), and WBC-EC adhesion, which may increase flow resistance by obstruction of the venular lumen

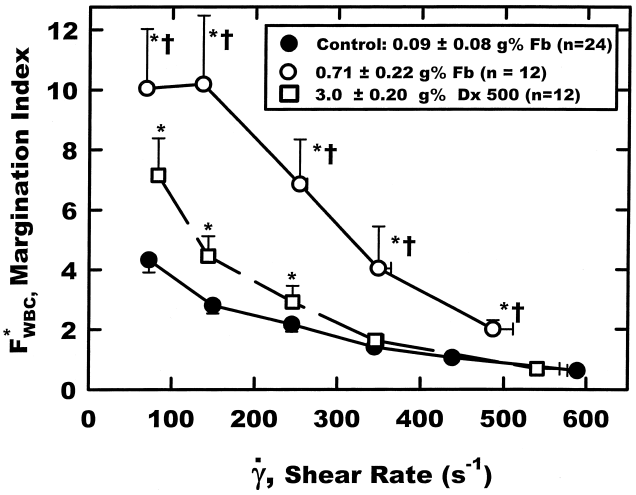

Figure 7. The margination of WBCs corresponding to the aggregation measurements of Figure 5 is presented in terms of the WBC rolling flux (F_{WBC}, cells/min), normalized with respect to its value in each of the 12 venules at high values of $\dot{\gamma} = 450\ s^{-1}$, i.e., $F^*_{WBC} = F_{WBC}/F_{WBC,\gamma=450}$. F^*_{WBC} increased exponentially with decreasing $\dot{\gamma}$ prior to fibrinogen infusion (●). Following fibrinogen infusion to achieve a plasma concentration of 0.71 g% (○) F^*_{WBC} increased 2-fold as $\dot{\gamma}$ was reduced to 150 s^{-1}, at which point a plateau was reached for further reductions. Also shown (dashed line) are the Dx500 (27) data for comparison. *Denotes a significant increase with Dx500, as assessed by the Mann–Whitney rank sum test ($p < .05$). †Significant difference between Dx500 and Fb data. Each point represents the mean ± SE.

(21). With regard to the latter, it appears logical to postulate that any rheological mechanism that prolongs the contact of WBCs with the venular EC may enhance the probability of forming an adhesive contact, as in the case of selectin mediated WBC rolling on the endothelium (20). Previously, it was shown that artificially inducing RCA with high molecular weight dextran (Dx500) enhances margination by maintaining rolling contact of WBCs on the EC (27). While RBCs may individually initiate the first contact of WBCs with the EC by the radial displacement of WBCs toward the vessel wall (30), the presence of red cell aggregates tends to inhibit the rapid remixing of WBCs into the central core, thus prolonging the margination process.

The role of RCA as a factor that enhances the resistance to flow is fraught with controversy. Although bulk viscosity increases with reductions in $\dot{\gamma}$, as studied by *in vitro* viscometry (5), the resistance to flow in small-bore tubes does not necessarily exhibit the same correlation. *In vitro* studies with glass tubes comparable in size to microvessels (28) have suggested that the apparent viscosity of blood may decrease with onset of RCA, presumably because of exclusion of aggregates from the tube entrance or their radial migration toward the axial core of the tube. In contrast, direct *in vivo* hemodynamic measurements in normal (23) and low-flow states (4) reveal a dramatic rise in apparent viscosity and increased resistance with reductions in shear rate. It has been suggested that the behavior of aggregates at the entrance to successive arteriolar bifurcations and venular confluences may be a source of increased resistance to explain the basis for this disparity. It has also been postulated that the increased viscosity that arises from RCA may be negated by the migration of red cell aggregates to the central axial core of small vessels (14). However, *in vivo* studies of the trajectories of red cell aggregates in venous vessels reveal that this effect is small and that a blunting of the velocity profile may be the dominant effect (14).

Resistance to Blood Flow

A major difficulty in studying the effects of RCA on the *in vivo* resistance to flow arises from the method for inducing RCA. The introduction of dextran (Dx) or other agents increases plasma viscosity as well and precludes attributing observed viscosity increases to RCA. In a previous study (27), infusion of Dx500 resulted in a 28% drop in V_{RBC} that was most likely caused by a 38% rise in bulk viscosity. To estimate the contribution of increased plasma viscosity to the flow reductions studied here, it was assumed that the viscosity of whole blood in arterioles was linearly related to H_{MICRO} by the relation, $\eta = aH_{MICRO} + \eta_0$, where $a = 0.04$ as determined *in vivo* (21). Using values of $\eta_0 = 1.2$ mPa s for rat plasma (35) and 0.96 mPa s for 0.74 g/100 mL fibrinogen (26), a 9% increase in blood viscosity was calculated to result from infusion of Fb. This value corresponds well with the 9% decrease observed for V_{RBC} (Figure 3), thus suggesting that the bulk viscosity rise is the principal cause of increased resistance and flow reductions, in contrast to hindrance of aggregate passage at branch points.

Fibrinogen vs. Dextran Aggregates

Within this framework, the 2-mediators of aggregation, Fb (Figure 1) and Dx (Figure 2), induce strikingly different degrees of RCA, with the former producing rouleaux and the latter clumps at the

concentrations used here. Although the mode of aggregate formation may be similar for both agents, and revolves around the forming of molecular cross-bridges between adjacent cells (6), the clumping induced by Dx suggests a stronger bond that is capable of deforming the RBC membrane to promote greater contact between opposing cells. The hydrodynamic consequences of rouleaux or clumps depend on the ease with which each enter the branches of the arteriolar bifurcations, as shown in Figures 1 and 2. It is evident from Figure 1 that weaker rouleaux are readily disrupted by their bending and distortion as they impinge upon the bifurcation, and easily enter the distal capillaries. In contrast, the Dx-induced clumps (Figure 2) may become more easily trapped, at the capillary entrance, as evidenced by the appearance of long, drawn-out tethers as aggregates are disrupted (Figure 2C). Although the precise dynamics of aggregate disruption for each case may be dependent on the length of time it takes to disrupt a given aggregate under similar pressure gradients, the greater systemic red cell trapping and reductions in venular H_{MICRO} induced by Dx (Figure 3) are consistent with its apparently greater strength of aggregation. This scenario is also supported by the dynamic measurements of the aggregation index G (Figure 6), where a 20% increase in G in venules for Fb was found as $\dot{\gamma}$ was reduced to 50 s^{-1}, in contrast to the corresponding 300% increase with Dx.

Leukocyte Margination

The dramatic increase in marginating WBC flux F^*_{WBC} observed in Figure 7 is consistent with 2 hemodynamic processes that may promote greater margination with Fb compared to Dx. First, the marked reduction in H_{MICRO} (Figure 3) and H_{SYS} (27) induced by Dx may lessen the ability of red cells to displace WBCs toward the venular wall. Margination in venules is largely independent of H_{MICRO} over a broad range, but it can be enhanced at extremely high H_{MICRO} (10) or may be absent at low H_{MICRO} (30). Second, the formation of clumps of RBCs with Dx may result in large gaps of plasma between aggregates that may serve to entrain WBCs and thus lessen the initial margination at the capillary exit, as illustrated in Figure 5.

It is also evident that with the introduction of Fb, a significant rise in WBC flux (Figure 7) occurs with no apparent increase in RCA (Figure 6) at high shear rates. This result may indicate a sensitivity of the index of aggregation G that may not be sufficient to detect small, yet influential, changes of RCA that affect WBC margination. Thus, the sensitivity of WBC radial migration to small changes in RCA may be substantially greater when rouleaux are present, as evidenced by the limited 20% rise in G with reductions in $\dot{\gamma}$. The illustrative video scenes of the extreme low-flow state (Figure 5) support this hypothesis.

Leukocyte-Endothelium Adhesion

The *in vivo* significance of Fb as a ligand for WBC–EC adhesion has yet to be fully explored. It has been shown that WBCs have receptors for Fb binding to the endothelium (1,16,17), and that fMLP-activated HL-60 cells infused into the rabbit mesentery increase their adhesiveness to the EC following exposure to Fb (31). The present experiments suggest that the addition of Fb or Dx results in a significant decrease in WBC rolling velocity and a significant increase in firm adhesion of WBCs and their marginating flux, at both high and low $\dot{\gamma}$ (Figure 4). For the WBC rolling velocity and firm adhesion, the effect of Dx on these indicators of WBC–EC adhesive interactions was significantly greater compared to Fb. Although the level of firm adhesion was significantly elevated, it remained at a very low level (on the order of 2 WBC/100 μm), which is dramatically less than levels routinely found in response to stimulated adhesion. Hence, although the slight increase in adhesion events and decrease in rolling velocity is consistent with a small increase in adhesiveness, it is unlikely that the dramatic increase in margination with Fb compared to Dx or control is a direct result of greater WBC–EC adhesion. This behavior most likely reflects the prolonged contact of WBCs with EC induced by the presence of RBC aggregates.

CONCLUSIONS

In summary, the elevation of circulating levels of fibrinogen dramatically increased WBC margination with reductions in shear rate. This trend arises from a small, yet significant increase in RCA whose effect on margination, compared to Dx, is magnified by maintenance of near normal levels of microvessel hematocrit. Although high molecular weight dextran may induce stronger and far greater levels of RCA, its effect on margination is diminished due to concomitant reductions in H_{MICRO}. Elevation of Fb also results in a small, yet significant increase in WBC-EC adhesion and a reduction in WBC rolling velocity that may result from its role as a ligand for Mac-1

and ICAM-1. Hence, because of its effect on RCA, increased fibrinogen has a synergistic effect on both margination and WBC–EC adhesive contact, which work together to promote firm adhesion of WBCs to the endothelium in the low-flow state.

REFERENCES

1. Altieri DC, Plescia J, Plow EF. (1993). The structural motif glycine 190–valine 202 of the fibrinogen gamma chain interacts with CD11b/CD18 integrin (alpha M beta 2, Mac-1) and promotes leukocyte adhesion. *J Biol Chem* 268:1847–1853.
2. Baker M, Wayland H. (1974). On-line volume flow rate and velocity profile measurement for blood in microvessels. *Microvasc Res* 7:131–143.
3. Blombäck B. (1996). Fibrinogen and fibrin-proteins with complex roles in hemostasis and thrombosis. *Clin Hemorheol* 16:383–477.
4. Cabel M, Meiselman HJ, Popel AS, Johnson PC. (1997). Contribution of red blood cell aggregation to venous vascular resistance in skeletal muscle. *Am J Physiol* 272:H1020–1032.
5. Chien S. (1975). Biophysical behavior of red cells in suspensions. In *The Red Blood Cell*, vol 2, 2nd ed., (D. MacN. Surgenor, Ed.). New York: Academic Press 1031–1133.
6. Chien S, Jan KM. (1973). Ultrastructural basis of the mechanism of rouleaux formation. *Microvasc Res* 5:155–166.
7. Coller BS. (1995). Blockade of platelet GPIIb/IIIa receptor as an antithrombotic strategy. *Circulation* 92:2373–2380.
8. Duperray A, Languino LR, Plescia J, McDowall A, Hogg N, Craig AG, Berendt AR, Altieri DC. (1997). Molecular identification of a novel fibrinogen binding site on the first domain of ICAM-1 regulating leukocyte–endotheolium bridging. *J Biol Chem* 272:435–441.
9. Ernst E. (1989). Fibrinogen, a cardiovascular risk factor. *Clin Hemorheol* 12:885–816.
10. Firrell JC, Lipowsky HH. (1989). Leukocyte margination and deformation in mesenteric venules of rat. *Am J Physiol* 256 (*Heart Circ Physiol* 25): H1667–H1674.
11. Goldsmith HL, Spain S. (1984). Margination of leukocytes in blood flow through small tubes. *Microvasc Res* 27:204–222.
12. Intaglietta M, Tompkins WR. (1973). Microvascular measurements by video image shearing and splitting. *Microvasc Res* 5:309–312.
13. Ivarsson L, Appelgren L, Rudenstam C-M. (1975). Plasma volume after dextran exchange in rats sensitive and nonsensitive to dextran. *Eur Surg Res* 7:315–325.
14. Johnson PC, Bishop JJ, Popel S, Intaglietta M. (1999). Effects of red cell aggregation on the venous microcirculation. *Biorheology* 36:457–460.
15. Kannel WB, Wolf PA, Castelli WP, D'Agostino RB. (1987). Fibrinogen and risk of cardiovascular disease. *JAMA* 258:1183–1186.
16. Languino LR, Plescia J, Duperray A, Brian AA, Plow EF, Geltosky JE, Altieri DC. (1993). Fibrinogen mediates leukocyte adhesion to vascular endothelium through an ICAM-1-dependent pathway. *Cell* 73:1423–1434.
17. Languino LR, Duperray A, Joganic KJ, Fornaro M, Thornton, GB, Altieri DC. (1995). Regulation of leukocyte–endothelium interaction and leukocyte transendothelial migration by intercellular adhesion molecule 1-fibrinogen recognition. *Proc Natl Acad Sci USA* 92:1505–1509.
18. Letcher RL, Chien S, Pickering TG, Sealey JE, Laragh JH. (1981). Direct relationship between blood pressure and blood viscosity in normal and hypertensive subjects: role of fibrinogen and concentration. *Am J Med* 70:1195–1202.
19. Lowe G, Rumley A, Norrie J, Ford I, Shepherd J, Cobbe S, Macfarlane P, Packard C. (2000). Blood rheology, cardiovascular risk factors, and cardiovascular disease: the West of Scotland Coronary Prevention Study. *Thromb Haemost* 84:553–558.
20. Ley K, Cerrito M, Arfors KE. (1991). Sulphated polysaccharides inhibit leukocyte rolling in rabbit mesentery venules. *Am J Physiol* 260:H1667–H1673.
21. Lipowsky HH, Usami S, Chien S. (1980). In vivo measurements of hematocrit and apparent viscosity in the microvasculature of cat mesentery. *Microvasc Res* 19:297–319.
22. Lipowsky HH, Usami S, Chien S, Pittman RN. (1982). Hematocrit determination in small bore tubes by differential spectrophotometry. *Microvasc Res* 24:42–55.
23. Mchedlishvili G, Gobejishvili L, Beritashvili N. (1993). Effect of intensified red blood cell aggregability on arterial pressure and mesenteric microcirculation. *Microvasc Res* 45:233–242.
24. Nobis U, Pries AR, Gaehtgens P. (1982). Rheological mechanisms contributing to WBC margination. In *Microcirculation Reviews*, I: *White Blood Cells—Morphology and Rheology as Related to Function* (Bagge U, Born GVR, Gaehtgens P, Eds). The Hague: Martinus Nijhoff, 57–65.
25. Park BH, Fikrig SM, Smithwick EM. (1968). Infection and nitrobluetetrazolium reduction by neutrophils. *Lancet* 2(7567):532–534.
26. Pearson MJ. (1996). *An Investigation into the Mechanisms of Rouleaux Formation and the Development of Improved Techniques for its Quantitation.* Thesis, University of London.
27. Pearson MJ, Lipowsky HH. (2000). Influence of erythrocyte aggregation on leukocyte margination in postcapillary venules of rat mesentery. *Am J Physiol* 279:1460–1471.

28. Reinke W, Gaehtgens P, Johnson PC. (1987). Blood viscosity in small tubes: effect of shear rate, aggregation and sedimentation. *Am J Physiol* 253:H540–H547.
29. Rampling MW, Gaffney PJ. (1976). The sulphite precipitation method for fibrinogen measurement; its use on small samples in the presence of fibrinogen degradation products. *Clin Chim Acta* 67:43–52.
30. Schmid-Schönbein, GW, Usami S, Skalak R, Chien S. (1980). The interaction of leukocytes and erythrocytes in capillary and postcapillary vessels. *Microvasc Res* 19:45–70.
31. Sriramarao P, Languino LR, Altieri DC. (1996). Fibrinogen mediates leukocyte–endothelium bridging in vivo at low shear forces. *Blood* 88:3416–3423.
32. Twersky V. (1970). Absorption and multiple scattering by biological suspensions. *J Opt Soc Am* 60:1084–1093.
33. Vejlens G. (1938). The distribution of leukocytes in the vascular system. *Acta Pathol Microbiol Scand* 33(Suppl):3–239.
34. Wayland H, Johnson PC. (1967). Erythrocyte velocity measurement in microvessels by a twoslit photometric method. *J Appl Physiol* 22:333–337.
35. Zingg W, Morgan CD, Anderson DE. (1971). Blood viscosity, erythrocyte sedimentation rate, packed cell volume, osmolality, and plasma viscosity of the wistar rat. *Lab Anim Sci* 21:740–742.